Mixing as an Aggregation Process

E. Villermaux[1,*] and J. Duplat[2]

[1]*Université de Provence & Institut Universitaire de France, IRPHE, 13384 Marseille Cedex 13, France*
[2]*Université de Provence, IUSTI, 13453 Marseille Cedex 13, France*

(Received 4 February 2003; published 31 October 2003)

Experiments show how a stirred scalar mixture relaxes towards uniformity through an aggregation process. The elementary bricks are stretched sheets whose rates of diffusive smoothing and coalescence build up the overall mixture concentration distribution. The cases studied, in particular, include mixtures in two and three dimensions, with different stirring protocols and Reynolds numbers which all lead to a unique family of concentration distributions stable by self-convolution, the signature of the aggregation mechanism from which they originate.

DOI: 10.1103/PhysRevLett.91.184501 PACS numbers: 47.10.+g, 47.27.–i

A mixture is a transient state between the initial segregation of the constituents and their ultimate homogeneity. The overall mixing process of a drop of dyed fluid in a stirred medium involves two phenomena: a process of dispersion of the drop in the diluting medium by which the phases interpenetrate, and a process of interaction between the dispersed elements from which homogeneity arises. We report in this Letter on findings suggesting that the nature of the interaction is of an aggregation type and that this phenomenon is the key to understanding the concentration distribution of a stirred mixture.

Let a jet of water plus a diluted fluorescent dye (disodium fluorecein) discharge in a square, transparent, long duct. For a given duct cross section, the injection diameter d and the velocity of the coflow at the entrance of the duct can be varied so that the average concentration of the dye in the channel $\langle C\rangle$ can be set at will. Since the cross section of the duct and the average velocity of the mixture in the downstream direction are constant, the average concentration is conserved. The jet velocity u is such that the Reynolds number $\mathrm{Re} = ud/\nu \simeq 10^4$.

The flow is made visual by means of a plane argon laser sheet slicing the duct along its axis, and as can be seen in Fig. 1, the dye rapidly invades the whole duct cross section, erasing its concentration differences as it travels downstream to relax towards a more or less uniform mixture.

After the dye has filled the channel cross section and evolves around a constant average concentration, the distribution $P(C)$ presents a skewed, bell shape which gets narrower around $\langle C\rangle$ in time (axial distances are converted to time through the average axial velocity with confidence as the radial velocity profile in a turbulent duct is flat [1]). The shape of $P(C)$ is very well described by a family of one parameter distributions, namely, gamma distributions

$$P(X = C/\langle C\rangle) = \frac{n^n}{\Gamma(n)} X^{n-1} e^{-nX}. \qquad (1)$$

The parameter n is adjusted at each downstream location for the gamma distribution of Eq. (1) to fit the experimental one. It is seen in Fig. 2 that the fairness of the fit holds for the whole concentration range, down to quite low probability levels, and accounts for the downstream deformation of $P(C)$ through the single parameter n, whose dependence on the downstream location is quite strong: Fig. 2 suggests a power-law dependence with an exponent close to $5/2$. The dependence of n on the jet Reynolds number is, although noticeable, very weak.

The stirring motions progressively convert a compact blob in a set of sheets of increasing surface and decreasing thickness [2–5]. The intersections of these sheets with the visualization plane are visible in Fig. 1 in the form of

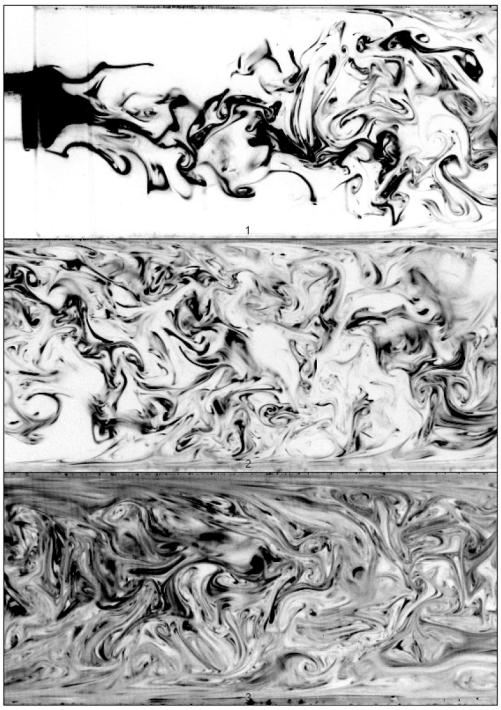

FIG. 1. Mixing of a dye discharging from a jet of diameter $d = 8$ mm in a square ($L \times L$ with $L = 3$ cm) duct. From 1 to 3, successive instantaneous planar cuts of the scalar field at increasing downstream locations in the duct showing the progressive uniformization of the dye concentration.

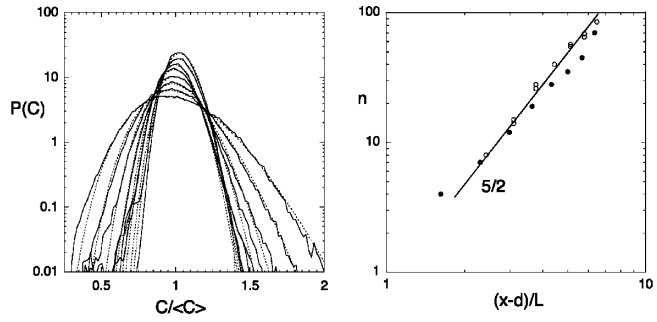

FIG. 2. Left: Downstream evolution of the concentration distribution $P(C)$ as the dye progresses along the duct as shown in Fig. 1. The concentration distribution of the evolving mixture gets narrower around the average concentration $\langle C\rangle = 0.3$. Solid line: experimental distributions; dashed line: distributions given by Eq. (1). Right: Fitting parameter n of the distributions (1) as a function of the downstream distance $(x-d)/L$. ○, Re $= 10^4$; ●, Re $= 5\times 10^3$.

ligaments. Let $s(t)$ be the distance between two material particles in the direction z perpendicular to a sheet, and $\sigma(t) = \partial \ln s(t)/\partial t$ its rate of compression. If $c(z, t)$ is the scalar concentration profile across the sheet, the convection-diffusion transport equation reduces to a one-dimensional problem provided the radius of curvature of the sheet is large compared to its thickness [6]. In that case the direction z aligns with the direction of maximal compression and for a species with diffusion coefficient D

$$\frac{\partial c(z,t)}{\partial t} + \sigma(t) z \frac{\partial c(z,t)}{\partial z} = D \frac{\partial^2 c(z,t)}{\partial z^2}. \tag{2}$$

By the change of variables $\tau = D\int_0^t dt'/s(t')^2$ and $\xi = z/s(t)$, Eq. (2) reduces [7–10] to a simple diffusion equation $\partial c(\xi,\tau)/\partial\tau = \partial^2 c(\xi,\tau)/\partial\xi^2$. The topology of the stirring motions select particular forms for $s(t)$. Starting with a sheet of initial uniform concentration and thickness s_0, the maximal concentration in $z = 0$ writes

$$c(0,t) = \mathrm{erf}(1/4\sqrt{\tau}) \overset{\tau\gg 1}{\longrightarrow} \frac{1}{\sqrt{\tau}}. \tag{3}$$

We describe several generic examples: in incompressible flows in two dimensions where the length of material lines grow like γt [11], the mean transverse thickness of the scalar filaments decreases as $s(t) = s_0/\sqrt{1+(\gamma t)^2}$ and thus $\tau = \frac{Dt}{s_0^2}[1 + \frac{(\gamma t)^2}{3}]$, providing $c(0,t) \sim (t/t_s)^{-3/2}$ for $t > t_s$, with $t_s \sim \frac{1}{\gamma}\mathrm{Pe}^{1/3}$, where $\mathrm{Pe} = \gamma s_0^2/D$ is a Péclet number. If material surfaces in three dimensions grow like $(\gamma t)^2$, then [12] $s(t) = s_0/[1+(\gamma t)^2]$ and $\tau = \frac{Dt}{s_0^2}[1 + \frac{2}{3}(\gamma t)^2 + \frac{1}{5}(\gamma t)^4]$, providing $c(0,t) \sim (t/t_s)^{-5/2}$ for $t > t_s$, with $t_s \sim \frac{1}{\gamma}\mathrm{Pe}^{1/5}$. For flows in which the length of material lines increases exponentially in time like $e^{\gamma t}$ as realized by a succession of stretching and folding motions in random flows [13], $s(t) = s_0 e^{-\gamma t}$ and $\tau = \frac{Dt}{s_0^2}(e^{2\gamma t} - 1)$ providing $c(0,t) \sim e^{-\gamma t}$ for $t > t_s$ with $t_s \sim \frac{1}{2\gamma}\ln\mathrm{Pe}$. These time scales are the relevant mixing times as soon as the inverse of the elongation rate γ^{-1} is smaller than the diffusive time of the sheet constructed on its initial size s_0^2/D, that is, for $\mathrm{Pe} \gg 1$. In this limit, t_s is essentially given by the time needed to deform the sheet γ^{-1} and pure diffusion [for which $c(0,t) \sim (Dt/s_0^2)^{-1/2}$] is enhanced by the substrate motion.

However, the sheets interact as they move in the flow so that their diffusive boundaries interpenetrate to give rise to new sheets whose concentration profile is the *addition* of the original ones. This elementary interaction rule is a consequence of the linearity of the Fourier diffusion Eq. (1) and dictates the kinetic evolution equation for $P(C, t)$. Let $Q(c, t)$ be concentration distribution of the elementary sheets and $\tilde{Q}(s,t) = \int_0^\infty Q(c,t)e^{-sc}dc$ its Laplace transform. The change of $Q(c,t)$ between t and $t + \Delta t$ is composed of two ingredients: First, the decay of c due to the stretching of the sheets results in a global shift of $Q(c,t)$ towards the low concentration levels without altering its shape as $-\frac{\partial}{\partial c}(\langle\frac{dc}{dt}\rangle Q)\Delta t = -\gamma\frac{\partial}{\partial c}(cQ)\Delta t$. Second, the sheets interact with nearby neighbors and because of the irregular stirring motions, the addition of the concentration levels is made at random among those available in the population $Q(c,t)$ at time t which therefore evolves, through this process, by self-convolution as $\int Q(c-c',t)Q(c',t)dc' = Q(c,t)^{\circledast 2}$. The time it takes to complete a convolution is the time needed to coalesce two sheets $\Delta t \approx \gamma^{-1} = -c(0,t)/(\frac{dc(0,t)}{dt})$; the continuous version of this convolution step thus writes in the Laplace space as $\tilde{Q}(s, t+\Delta t) = (1-\gamma\Delta t)\tilde{Q}(s,t)^{1-\gamma\Delta t} + \gamma\Delta t\tilde{Q}(s,t)^2 + \mathcal{O}((\gamma\Delta t)^2)$ which both leaves $\tilde{Q}(s,t)$ unchanged for $\Delta t = 0$ and provides $\tilde{Q}(s, t+\gamma^{-1}) \equiv \tilde{Q}(s,t)^2$. Taking the limit $\Delta t \to 0$, the global rate of change of $\tilde{Q}(s,t)$ accounting for the two ingredients is thus given by

$$\frac{\partial\tilde{Q}}{\partial t} = -\gamma s\frac{\partial\tilde{Q}}{\partial s} + \gamma(-\tilde{Q} + \tilde{Q}^2 - \tilde{Q}\ln\tilde{Q}). \tag{4}$$

The above interaction rule leads, irrespective of the initial condition for $Q(c,0)$, to decaying exponential distributions [14] of mean $\langle c\rangle = c(0,t)$ as defined in Eq. (3). The concentration C results from clusters of several of these interacting sheets. If these clusters are made of n independent coalesced sheets, then the distribution of the concentration $P(C,t)$ is the nth convolution of $Q(c,t)$, that is, $\tilde{P}(s,t) = \tilde{Q}(s,t)^n$, whose overall kinetic equation derives from Eq. (4) as

$$\frac{\partial\tilde{P}}{\partial t} = -\gamma s\frac{\partial\tilde{P}}{\partial s} + \gamma n(-\tilde{P} + \tilde{P}^{(1+1/n)}) + \left(\frac{1}{n}\frac{dn}{dt} - \gamma\right)\tilde{P}\ln\tilde{P}. \tag{5}$$

With $\gamma n = \frac{dn}{dt}$, the asymptotic solution of Eq. (5) is $\tilde{P} = (1 + \langle C\rangle\frac{s}{n})^{-n}$, providing a gamma distribution of order n for $P(C,t)$, that is, a convolution of n exponentials. The

average concentration $\langle C \rangle$ of the mixture is conserved when the damping factor γ balances exactly the coalescence rate, that is, when $n = 1/c(0, t)$. This condition is realized provided $n \sim (t/t_s)^{5/2}$ in this three-dimensional flow, as expected from Fig. 2 [15].

By changing the dimensionality of the flow from three to two, it is expected that as long as the stirring motions are sufficiently irregular to ensure an addition of the concentration levels at random, the distribution is, as in the three-dimensional case, generated by self-convolution. It is, by contrast, also expected that the dependence of n on time will be different. We illustrate this difference on hand of a simple experiment consisting of stirring a blob of dye with a rod in a thin layer of a very viscous fluid, by a two-dimensional quasiperiodic protocol which mimics the motion of a straw in a milk shake. The diluting fluid is pure glycerol, and the drop is made of the same fluid colored with india ink. A number of parallel cuts are made in one direction, and then the same number at right angles, this operation defining one cycle (Fig. 3).

In this low Reynolds number flow (the typical Reynolds number of the motion of the rod is $\mathrm{Re} = us_0/\nu = 10^{-1}$), the fluid is deformed by the passage of the rod on a scale which is given by its own size s_0. The length of material lines is equal to the distance traveled by the rod in the medium, and it is actually observed that the net contour length of the deformed scalar drop increases in proportion to the number of cycles (Fig. 4). The mixing time, or, alternatively, the number of cycles p needed to start mixing the drop in the surrounding medium is thus, since $L/L_0 = 1 + \gamma t \approx 1 + 17.5 \times p$, given by $\gamma t_s \approx 17.5 \times p_s \sim (\gamma s_0^2/D)^{1/3} = (\mathrm{Re}Sc)^{1/3}$ with $\gamma \approx u/s_0$ the typical elongation rate, $u \approx 4.6$ cm/s the rod velocity, giving, with $s_0 \approx 2$ mm and $Sc \approx 10^6$, a mixing cycle p_s of the order of 2.5 (see Fig. 4).

The maximal rate of stretch is obtained for fluid particles close to the rod trajectory, while the protocol leaves nearly unstretched fluid parcels which therefore keep a concentration close to the initial concentration as the number of cycles is increased. Concomitantly, fluid particles are brought together in the wake of the rod and coalesce. The amplitude of the slicing movements is constant through the cycles, so that the average concentration of the dye must be conserved; these are the ingredients required for the aggregation scenario we have described to occur. The distributions displayed on Fig. 5 are actually reasonably well described by the gamma functions family of Eq. (1) with an average concentration $\langle C \rangle$ constant. The maximal concentration in each single scalar filament decreases as $c(0, t) \sim (t/t_s)^{-3/2}$ and the orders of the gamma distributions consistently follow $n \sim (\text{number of stirring cycles})^{3/2}$ in this two-dimensional flow.

As soon as a mixture is stirred in a more or less irregular manner, the addition is made at random among

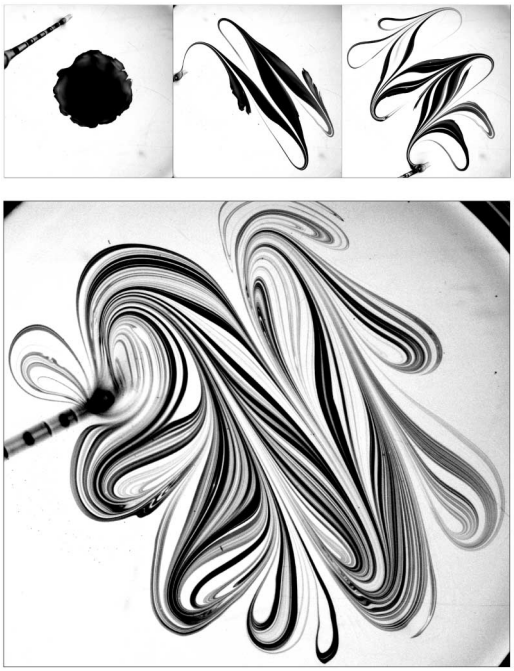

FIG. 3. Top: The stirring protocol of a drop of ink deposed at the surface of pure glycerol using a small rod. The sequence displays the initial state, half, and a completed stirring cycle. Bottom: The mixture's state after $2\frac{1}{2}$ completed stirring cycles.

the levels available in the current distribution. This operation implies that the concentration distribution evolves by self-convolution and, when it actually does, gives an *a posteriori* precise definition of what "random" means. This process, which basically amounts to a convolution of exponentials [16–20], might certainly be generic of the construction mechanism of the skewed distributions with exponential tails widespread in various instances including turbulent convection [21], grid turbulence [22,23],

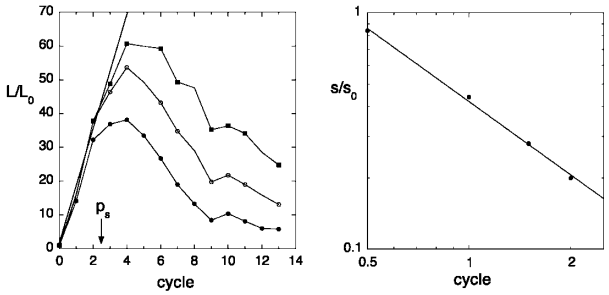

FIG. 4. Left: Contour length of the drop as it deforms through the mixing cycles for three different concentration thresholds. The length increases linearly independently of the concentration thresholds chosen to define the contour up to the mixing cycle $p_s \approx 2.5$. For $p > p_s$, the contour length depends on the concentration threshold and, at fixed threshold, decreases as p increases. Right: Corresponding average transverse sheet, or striation thickness s before the mixing cycle; the line has a slope -1.

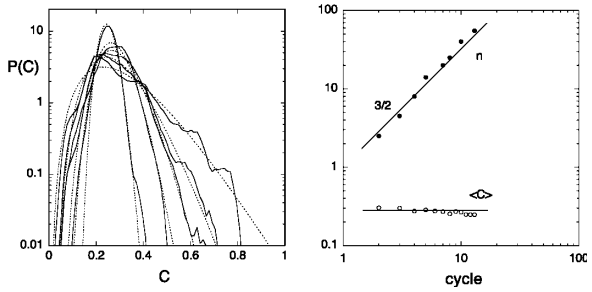

FIG. 5. Left: Evolution of the dye concentration distribution $P(C)$ after 3, 4, 5, 6 and 13 cycles according to the protocol shown on Fig. 3. The concentration distribution of the evolving mixture gets narrower around the average concentration $\langle C \rangle$. solid line: experimental distributions, dashed line: distributions given by Eq. (1). Right: Fitting parameter n and average concentration of the distributions (1) as a function of the number of cycles.

shear layers [12], randomly stirred two-dimensional flows [24–26], or jets [27]. This scenario not only accounts for the distributions tail [28–31], but for their *whole* shape and evolution.

It is finally instructive to note that an experiment performed at a very low Reynolds number produces composition fields very similar to those obtained at a much larger Reynolds number (Figs. 2 and 5). The reason is that the evolution mechanism is the same. The motion of the rod in the two-dimensional viscous fluid plays the role of the random stirring motions present in high Reynolds number flows. Their role is to ensure the independence—in the statistical sense of Eq. (5)—of the addition of the concentration levels; a particularly simple paradigm for the impact of turbulence on mixing.

*Email address: villerma@irphe.univ-mrs.fr

[1] H. Schlichting, *Boundary Layer Theory* (McGraw-Hill, Inc., New York, 1987).
[2] O. Reynolds, Nature (London) **50**, 161–164 (1894).
[3] J. M. Ottino, Phys. Fluids A **3**, 1417–1430 (1991).
[4] S. S. Girimaji and S. B. Pope, J. Fluid Mech. **220**, 427–458 (1990).
[5] J. Duplat and E. Villermaux, Eur. Phys. J. B **18**, 353–361 (2000).
[6] P. E. Dimotakis and H. J. Catrakis, in *Mixing: Chaos and Turbulence*, H. Chaté, E. Villermaux, and J. M. Chomaz (Kluwer Academic/Plenum Publishers, New York, 1999).
[7] W. E. Ranz, AIChE J. **25**, 41–47 (1979).
[8] F. E. Marble, in *Chemical Reactivity in Liquids: Fundamental Aspects*, edited by M. Moreau and P. Turq (Plenum Press, New York, 1988).
[9] C. J. Allègre and D. L. Turcotte, Nature (London) **323**, 123–127 (1986).
[10] J. M. Ottino, *The Kinematics of Mixing: Stretching, Chaos, and Transport* (Cambridge University Press, Cambridge, 1989).
[11] P. Meunier and E. Villermaux, J. Fluid Mech. **476**, 213–222 (2003).
[12] E. Villermaux and H. Rehab, J. Fluid Mech. **425**, 161–185 (2000).
[13] G. K. Batchelor, Proc. R. Soc. London, Ser. A **213**, 349–366 (1952).
[14] S. K. Friedlander, *Smoke, Dust, and Haze* (Oxford University Press, New York, 2000).
[15] This apparent power law is a transient effect reflecting the fact that the temporal window of the mixture's evolution covers, at most, a few large scale turnover times $\gamma^{-1} \sim L/u'$. Indeed, material lines increase like $L/L_0 = \exp(\gamma t) = \exp(u't/L) = \exp(u'/u \times x/L)$ where $x = ut$ is the distance from the injection point of the scalar blob in the medium advected at a velocity u. In the channel flow, the turbulence intensity is such that [1] $u'/u \approx 0.08$ and the downstream distances of observation in the present experiments are such that $x/L < 10$ so that $L/L_0 \approx 1 + u'/u \times x/L = 1 + \gamma t$, realizing in practice an elongation linear in time, inducing, in this three-dimensional flow, $n \sim t^{5/2}$. This behavior has thus to be understood as the birth of the ultimate exponential regime, but this slight difference, if any, has strictly no consequence on the mechanism building up the concentration distribution $P(C)$ which solely relies on *random additions* of concentration levels, independently of the *rate* at which these additions are made.
[16] W. Feller, *An Introduction to Probability Theory and Its Applications* (John Wiley & Sons, New York, 1970).
[17] M. von Smoluchowski, Z. Phys. Chem. **92**, 129–168 (1917).
[18] R. L. Curl, AIChE J. **9**, 175–181 (1963).
[19] A. Pumir, B. I. Shraiman, and E. D. Siggia, Phys. Rev. Lett. **66**, 2984–2987 (1991).
[20] S. B. Pope, Prog. Energy Combust. Sci. **11**, 119–192 (1985).
[21] B. Castaing, G. Gunaratne, F. Heslot, L. Kadanoff, A. Libchaber, S. Thomae, X. Z. Wu, S. Zaleski, and G. Zanetti, J. Fluid Mech. **204**, 1–30 (1989).
[22] Jayesh and Z. Warhaft, Phys. Fluids A **4**, 2292–2307 (1992).
[23] S. T. Thoroddsen and C. W. Van Atta, J. Fluid Mech. **244**, 547–566 (1992).
[24] B. S. Williams, D. Marteau, and J. P. Gollub, Phys. Fluids **9**, 2061–2080 (1997).
[25] M. C. Jullien, P. Castiglione, and P. Tabeling, Phys. Rev. Lett. **85**, 3636–3639 (2000).
[26] M. Holzer and E. D. Siggia, Phys. Fluids **6**, 1820–1837 (1994).
[27] E. Villermaux, C. Innocenti, and J. Duplat, Phys. Fluids **13**, 284–289 (2001).
[28] B. I. Shraiman and E. D. Siggia, Phys. Rev. E **49**, 2912–2927 (1994).
[29] B. I. Shraiman and E. D. Siggia, Nature (London) **405**, 639–646 (2000).
[30] G. Falkovich, K. Gawedzki, and M. Vergassola, Rev. Mod. Phys. **73**, 913–975 (2001).
[31] E. Balkovsky and A. Fouxon, Phys. Rev. E **60**, 4164–4174 (1999).